Limnol. Oceanogr., 51(1), 2006, 310–320

Coccolith strontium to calcium ratios in *Emiliania huxleyi:* The dependence on seawater strontium and calcium concentrations

Gerald Langer[1]
Alfred Wegener Institute for Polar and Marine Research, Am Handelshafen 12, 27570 Bremerhaven, Germany

Nikolaus Gussone
Research Centre Ocean Margins, University of Bremen, P.O. Box 330440, D-28334 Bremen, Germany

Gernot Nehrke
Alfred Wegener Institute for Polar and Marine Research, Am Handelshafen 12, 27570 Bremerhaven, Germany

Ulf Riebesell
Marine Biogeochemistry, Leibniz Institute for Marine Sciences, University of Kiel, Düsternbrooker Weg 20, 24105 Kiel, Germany

Anton Eisenhauer
Marine Biogeochemistry, Leibniz Institute for Marine Sciences, University of Kiel, Wischhofstraße 1-3, 24148 Kiel, Germany

Henning Kuhnert
Research Centre Ocean Margins, University of Bremen, P.O. Box 330440, D-28334 Bremen, Germany

Björn Rost
Alfred Wegener Institute for Polar and Marine Research, Am Handelshafen 12, 27570 Bremerhaven, Germany

Scarlett Trimborn
Alfred Wegener Institute for Polar and Marine Research, Am Handelshafen 12, 27570 Bremerhaven, Germany

Silke Thoms[1]
Alfred Wegener Institute for Polar and Marine Research, Am Handelshafen 12, 27570 Bremerhaven, Germany

Abstract

In recent studies the Sr/Ca ratio of coccolithophore calcite was used as a proxy for past coccolithophore growth and calcification rates. Since Sr and Ca concentrations in seawater have not remained constant through time, interpretation of Sr/Ca data from the coccolith-dominated sedimentary record requires knowledge about the incorporation of seawater Sr into coccolith calcite during coccolithogenesis. Here we show that Sr/Ca of *Emiliania huxleyi* coccoliths is linearly related to seawater Sr/Ca, meaning that the Sr exchange coefficient does not change with changing seawater Sr/Ca. The exchange coefficient for Sr in this study, 0.39, is close to values presented in the literature and is high compared with values obtained by inorganic precipitation experiments. This suggests a strong effect of cell physiology on biogenic calcite precipitation in coccolithophores. We present a conceptual model, based on the transmembrane transport of Sr and Ca, which explains the offset.

[1] Corresponding authors (glanger@awi-bremerhaven.de, sthoms@awi-bremerhaven.de).

Acknowledgments

We gratefully acknowledge the assistance of Anja Terbrüggen and Christiane Lorenzen in the laboratory. We thank Jeremy Young and Karen Henriksen for providing valuable insights into coccolithophore calcification. Special thanks go to Heather Stoll whose careful comments greatly improved the manuscript. G. L. acknowledges the financial support of NEBROC (Netherlands Bremen Oceanography Science Co-Operation in Marine Research). This work was supported by the German Research Foundation (DFG) and is part of the projects TH 744/2-1, BI 432/3-2, and the DFG Research Center ''Ocean Margins'' of the University of Bremen (RCOM0322). This study is a contribution to the ESF project CASIOPEIA (Ei272/17-1, O4ECLIM_FP08).

The Sr/Ca of calcium carbonate–producing organisms was widely used to reconstruct past oceanographic conditions. Coral Sr/Ca, for instance, was used as a temperature proxy (Smith et al. 1979). Sr/Ca of coccolithophore calcite was linked to coccolithophore growth and calcification rates (Stoll and Schrag 2000). It was suggested that despite temperature-dependent Sr/Ca partitioning in coccolith calcite (Stoll et al. 2002*a*,*b*), it is possible to infer past coccolithophore productivity from the coccolith fossil record (Stoll and Schrag 2001; Billups et al. 2004).

The Sr/Ca of seawater is likely to have changed through time on both short and long timescales (Stoll and Schrag 1998; Lear et al. 2003). Therefore, it is mandatory to consider its influence on the Sr/Ca of biogenic calcium carbonates. Recent studies investigating coccolith-dominated Cenozoic and Cretaceous carbonates consequently account for changing seawater Sr/Ca (Stoll and Schrag 2001; Billups et al. 2004). Calculations in these studies rely on the premise that the exchange coefficient is unaffected by the seawater Sr/Ca ratio. This was shown to be true in inorganically precipitated calcite (Lorens 1981; Tesoriero and Pankow 1996), whereas nothing is known about coccolithophores in this respect.

Exchange coefficients of coccolith calcite presented in the literature are high compared with values of inorganically precipitated calcite (Stoll et al. 2002*b*). Although kinetic effects can explain part of this offset (Stoll et al. 2002*b*), the origin of this discrepancy is yet not fully understood. Often the term ''vital effects'' is used to account for the fact that numerous biological processes control the precipitation process. Because the bulk of the coccolith is thought to be precipitated by an inorganic crystal growth mechanism (Young et al. 1999), the application of results from inorganic precipitation experiments to coccolithogenesis may provide a useful framework. However, such inferences are doubtful, because precipitation of coccolith calcite takes place within a specialized Golgi-derived vesicle—the so-called coccolith-vesicle—and is organically modulated (Young et al. 1999; Henriksen et al. 2004). Determination of exchange coefficients for coccoliths is problematic, because the Sr/Ca of seawater is used for calculation, although the chemistry of seawater differs from that of the solution within the coccolith vesicle.

Here we present results from batch culture experiments using the dominant coccolithophore *Emiliania huxleyi*, a bloom-forming species that occurs worldwide in both coastal and open oceanic environments. In these experiments the dependence of coccolith Sr/Ca on seawater Sr/Ca was examined. Our results are compared with literature data, and a conceptual model for transport of calcium and strontium from seawater into the coccolith-vesicle, capable of explaining the observed high values of exchange coefficient, is discussed. (Notations used within this paper are listed in Table 1.)

Table 1. Notation.

d	Day
D_x	Partition coefficient for the element x
$K_{D_{Sr}}$	Exchange coefficient for Sr
$K_{D_{Tr}}$	Exchange coefficient for a trace element (Tr)
$K^B_{D_{Tr}}$	Apparent exchange coefficient for a trace element (Tr)
K_{MCO3}, K_{TrCO_3}	Solubility product of MCO_3 and $TrCO_3$, respectively
K_{sp}	Seawater calcite saturation product
R	Gas constant
T	Absolute temperature
γ_{Tr}/γ_M	Ratio of activity coefficients for trace (Tr) and major (M) element in solution
$\Delta\mu$	Difference of the chemical potential of the trace element in the pure $TrCO_3$ and in the MCO_3
ν_a	Stochiometry factor accounting for the number of anions in the carbonate structure
ν_c	Stochiometry factor accounting for the number of cations in the carbonate structure
Ω	Calcite supersaturation

Materials and Methods

Monospecific cultures of *E. huxleyi* (strain PML B92/11) were grown in sterile-filtered (0.2 μm) artificial seawater enriched with 100 μmol L^{-1} nitrate and 6.25 μmol L^{-1} phosphate with trace metals and vitamins according to F/2 (Guillard and Ryther 1962). The detailed composition of the artificial seawater is given in Table 2. Seawater Sr and Ca concentrations were varied to obtain a wide range in Sr/Ca in the growth medium. A 16 : 8 light : dark (LD) cycle was applied. Experiments were carried out at a constant temperature of 15°C and various photon flux densities (Table 3), which were maintained by growing the cells in an adjustable incubator (Rubarth Apparate GmbH, Germany). Cells were pre-adapted to experimental conditions for approximately 12 generations and grown in dilute batch cultures. Low cell density at harvest ensured that <5% dissolved inorganic carbon (DIC) was consumed (i.e., DIC consumed by the cells at the end of experiment). The carbonate system was nearly constant during all experiments and did not vary significantly between different flasks. CO_2 concentrations [CO_2] were adjusted to an average value of 16.4 μmol L^{-1} through the addition of NaOH (1 mol L^{-1}). The cells were grown in duplicate in HCl-rinsed polycarbonate flasks.

Samples for alkalinity measurements were filtered (approximately 0.6 μm), poisoned with 1 mL of an $HgCl_2$ solution (35 g L^{-1}), and stored in 300-mL borosilicate flasks

Table 2. Composition of artificial seawater.

Salt	Reagent grade, producer	Final concentration (mmol L^{-1})
NaCl	Suprapur, Merck	395
$MgCl_2 \times 6H_2O$	Fractopur, Merck	53.23
Na_2SO_4	Suprapur, Merck	28.24
KCl	Fractopur, Merck	10
$SrCl_2 \times 6H_2O$	P.A., Merck	0.004, 0.02, 0.09, 0.42
$NaHCO_3$	Suprapur, Merck	2.33
NaBr	Suprapur, Merck	0.84
H_3BO_3	Suprapur, Merck	0.4
$CaCl_2 \times 4H_2O$	Suprapur, Merck	1, 10, 20

Table 3. Experimental setup and results.

Experiment No.	PFD (μmol m^{-2} s^{-1})	$[Ca]_B$ (mmol L^{-1})	$[Sr]_B$ (mmol L^{-1})	Seawater Sr/Ca (mmol mol^{-1})	Coccolith Sr/Ca (mmol mol^{-1})	Apparent Sr exchange coefficient	Growth rate μ_{cocco} (d^{-1})	Calcification rate (pg calcite cell^{-1} d^{-1})
1	100	1	0.09	90	37	0.411	0.54	8
2	100	10	0.09	9	5.44	0.605	0.86	23
3	100	20	0.09	4.5	2.67	0.592	0.86	24
4	300	1	0.09	90	37	0.411	0.66	5
5	300	10	0.09	9	5.48	0.608	0.85	26
6	300	20	0.09	4.5	2.67	0.594	0.78	22
7	500	1	0.09	90	36.2	0.402	0.65	3
8	500	10	0.09	9	5.63	0.625	0.89	26
9	500	20	0.09	4.5	2.9	0.645	0.91	29
10	800	1	0.09	90	33.8	0.376	0.71	2
11	800	10	0.09	9	5.32	0.591	0.87	25
12	800	20	0.09	4.5	2.6	0.578	0.77	24
13	30	10	0.004	0.4	0.17	0.427	0.56	18
14	30	10	0.02	2	0.64	0.320	0.53	17
15	30	10	0.42	42	13.7	0.325	0.55	17
16	300	10	0.004	0.4	0.16	0.390	0.87	55
17	300	10	0.02	2	0.68	0.340	0.80	51
18	300	10	0.42	42	15.2	0.363	0.87	58

at 0°C. DIC samples were sterile-filtered (0.2 μm) and stored in 13-mL borosilicate flasks free of air bubbles at 0°C prior to analysis. Total alkalinity was calculated from linear Gran plots (Gran 1952) after duplicate potentiometric titration (Bradshaw et al. 1981; Brewer et al. 1986), and DIC was measured photometrically (Stoll et al. 2001) in triplicates. The carbonate system was calculated from temperature, salinity, concentrations of DIC, total alkalinity, and phosphate using the program CO_2sys (Lewis and Wallace 1998). Equilibrium constants of Mehrbach et al. (1973) refitted by Dickson and Millero (1987) were chosen. Samples for determination of total particulate carbon (TPC) and particulate organic carbon (POC) were filtered on precombusted (12 h, 500°C) GF/F-filters (approximately 0.6 μm) and stored at −20°C. Prior to analysis, the POC filters were fumed for 2 h with a saturated HCl solution to remove all inorganic carbon. TPC and POC were subsequently measured on a Carlo Erba NA-1500 Analyzer. Particulate inorganic carbon (PIC) was calculated as the difference between TPC and POC. For determination of cell density, samples were taken daily or every other day and counted immediately after sampling using a Coulter Multisizer III. Cell growth rate (μ_{cocco}, unit d^{-1}) was calculated as

$$\mu_{cocco} = (\ln c_1 - \ln c_0)/\Delta t \quad (1)$$

where c_0 and c_1 denote the cell densities at the beginning and the end of experiment, and Δt represents the duration of incubation in days.

Calcification rate (P, pg calcite cell^{-1} d^{-1}) was calculated according to

$$P = \mu_{cocco} \times (\text{cellular calcite content}) \quad (2)$$

Samples for Sr/Ca measurements were centrifuged in 50-mL Falcon tubes, rinsed with Sr-free artificial seawater, centrifuged again in 1-mL tubes in order to remove seawater, dried at 60°C for 48 h, and stored at room temperature.

Sample preparation and determination of Sr/Ca ratios—Coccolith samples were transferred into acid-cleaned 1.5-mL polypropylene (PP) polymerase chain reaction (PCR) tubes. For removal of organic matter, the samples were bleached in a 10% dilution of concentrated NaOCl solution for about 24 h. Afterward the solution was removed and the samples were covered with ultrapure H_2O (pH 8–9, adjusted by the addition of NH_4OH to prevent partial dissolution of the calcite samples); ultrasonicated for 2 min; and then centrifuged. The water was removed and new H_2O was added. This washing procedure was repeated 6 times. The cleaned coccoliths were dissolved in 2.5 mol L^{-1} HCl and evaporated. The samples were recovered in an HNO_3–H_2O_2 mixture and evaporated again. The samples were recovered in 2% HNO_3, and internal Sc and Y standards were added prior to element analysis. Ca and Sr concentrations were determined on a Finnigan Element 2 inductively coupled plasma mass spectrometer at the Department of Geosciences at the University of Bremen. The reproducibility (2 standard deviations) of the Sr/Ca ratios was determined to be about 0.038 mmol mol^{-1} by repeated measurements of a house standard during the course of the analyses.

Theoretical background—The partition coefficient describes the distribution of an element between two phases. In aqueous systems these two phases are normally an aqueous solution and a mineral. Unfortunately, the terminology in this field is incoherently used throughout the literature (Beattie et al. 1993), so that the terms ''partition coefficient,'' ''distribution coefficient,'' and ''exchange coefficient'' and the symbols D, K_d, and K_D are used interchangeably. We use the following terminology: The partition coefficient and the symbol D_x (the subscript x stands for the element of interest) are defined as

$$D_x = \frac{[x]_s}{[x]_l} \quad (3)$$

where $[x]_s$ is the molar concentration of the element of interest in the solid and $[x]_l$ its molar concentration in the solution. For most aqueous systems the partition coefficient is normalized to the partition coefficient of another element. The term exchange coefficient and the symbol $K_{D_{Tr}}$ will be used for the normalized value. From here on the subscript *Tr* (trace element) and *M* (major element) will be used instead of the previously used *x*, because this is more consistent with the literature. The exchange coefficient is defined as

$$K_{D_{\mathrm{Tr}}} = \frac{D_{\mathrm{Tr}}}{D_M} \quad (4)$$

D_{Tr} is the partition coefficient of the element of interest, and D_M is the partition coefficient of the element used for normalization. Since in this work we focus on the element strontium (Sr), the exchange coefficient for Sr is defined as the partitioning of Sr between calcite and the solution normalized to the distribution of calcium (Ca) between calcite and solution (Eq. 5).

$$K_{D_{\mathrm{Sr}}} = \frac{[\mathrm{Sr}]_S/[\mathrm{Sr}]_l}{[\mathrm{Ca}]_S/[\mathrm{Ca}]_l} \quad (5)$$

It has been shown that the distribution of trace elements at thermodynamical equilibrium is related to the solubility product of the mineral phases. McIntire (1963) showed that the solubility products of MCO_3 and $TrCO_3$ are correlated to the exchange coefficient as follows (see Table 1 for symbol explanations):

$$K_{D_{\mathrm{Tr}}} = \left(\frac{K_{\mathrm{MCO_3}}}{K_{\mathrm{TrCO_3}}}\right)^{1/\nu_c} \left(\frac{\gamma_{\mathrm{Tr}}}{\gamma_M}\right) \left[\exp\left(\frac{-\Delta\mu}{\nu_a RT}\right)\right] \quad (6)$$

It is difficult to measure or calculate the values for all parameters of this equation. In particular, the difference of the chemical potential of the trace element in the pure $TrCO_3$ crystal and its chemical potential as a component in the MCO_3 crystal is not known. Rimstidt et al. (1998) tried to estimate the values for various elements by fitting a large data set obtained from the literature. Their work, and many other experimental investigations (e.g., Lorens 1981; Tesoriero and Pankow 1996), showed that the exchange coefficient is in many cases influenced by kinetics. The degree of supersaturation has a strong influence on the growth processes at the crystal surface, which are complex and not trivial to investigate. However, the crystal growth rate generally increases with increasing levels of supersaturation (Nielsen 1964). Experiments with varying growth rates are easily performed and therefore ideal for the investigation of the kinetic effects on trace element incorporation during crystal growth. Numerous experiments showed that three different exchange behaviors of trace elements can be distinguished (e.g., Tesoriero and Pankow 1996; Rimstidt et al. 1998): (1) the trace element concentration is enriched within the crystal compared with its concentration in solution, $K_{D_{Tr}}$; (2) the trace element concentration is depleted within the crystal, $K_{D_{Tr}} < 1$; and (3) no fractionation occurs, $K_{D_{Tr}} = 1$.

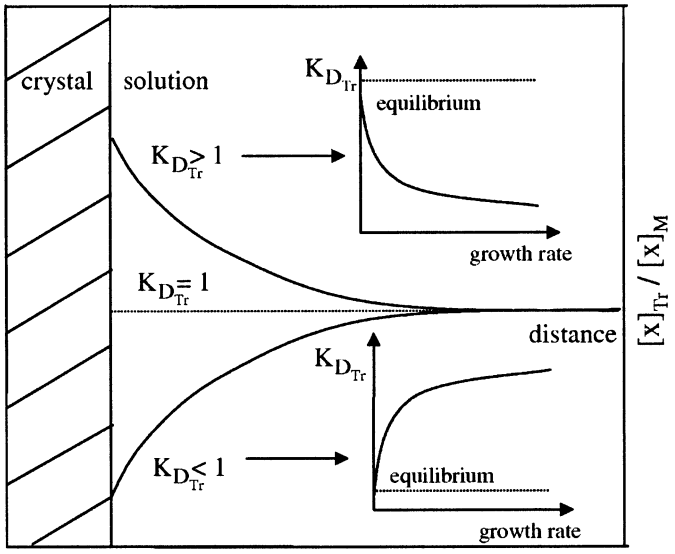

Fig. 1. Dependence of the exchange coefficient $K_{D_{Tr}}$ on the element ratio x_{Tr}/x_M in the bulk medium. For a $K_{D_{Tr}} > 1$, the value for x_{Tr}/x_M is higher in the crystal than the bulk value. A $K_{D_{Tr}}$ value < 1 shows the opposite exchange behavior. If the incorporation into the crystal shows the same ratio as the bulk medium, the $K_{D_{Tr}} = 1$. For $K_{D_{Tr}}$ values τ 1, experimental values are in general lower than the predicted equilibrium value and approaches equilibrium values with decreasing growth rate. The opposite holds for experimental values in the case of $K_{D_{Tr}} < 1$. (Modified after Rimstidt et al. 1998.)

Depending on this exchange behavior, the measured value for the exchange coefficient differs from the estimated equilibrium value in the following way. For elements with a $K_{D_{Tr}} > 1$, measured $K_{D_{Tr}}$ values are lower than predicted and approach the predicted value with decreasing growth rate. For $K_{D_{Tr}} < 1$, the opposite behavior can be observed. This behavior is illustrated in Fig. 1. It should be noted that, strictly speaking, equilibrium is only achieved under conditions of zero growth. In spite of this, the term ''growth at equilibrium'' is widely used in the literature and describes a behavior not influenced by kinetics. However, for our purposes it is important to note that the concentration measured within the crystal can be influenced by two variables: the concentration in solution (Eq. 3) and the growth rate of the crystal. The concentration in solution in general refers to the solution the crystal is precipitated from. If crystal growth proceeds via biomineralization, the chemical composition of the fluid at the actual growth site, located within an organism, is mostly unknown. Nevertheless, it is common to calculate an exchange coefficient by means of the element ratio in the growth medium (bulk medium). Values obtained in this way are not based on the real composition at the site of crystal growth. We suggest that exchange coefficients calculated based on a reference solution (if the solution composition at the site of crystal growth is not known) should be referred to as apparent exchange coefficient, $K^B_{D_{Tr}}$ (the superscript *B* denotes the use of the bulk medium concentration as the

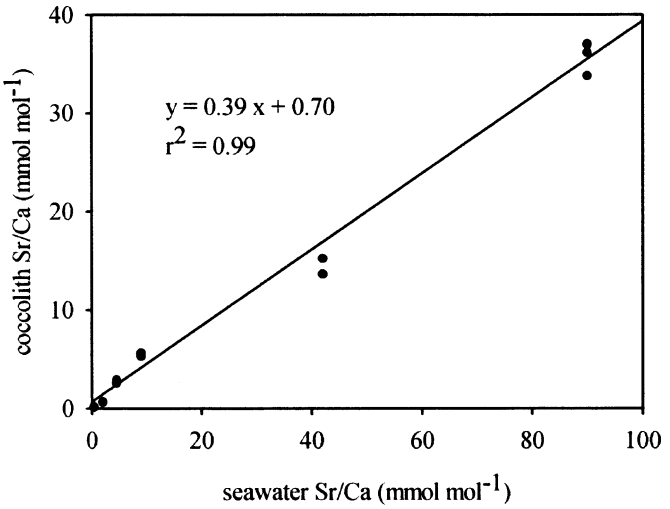

Fig. 2. Experimental results. Shown is the dependence of Sr/Ca in coccolith calcite on Sr/Ca in bulk medium. The slope of the linear regression curve yields a $K^{B}_{D_{Sr}}$ of 0.39.

reference solution). Symbol explanations are given in Table 1.

Results

The Sr/Ca of coccolith calcite is linearly related to Sr/Ca of seawater (Fig. 2). The slope of the regression curve (Fig. 2) represents $K^{B}_{D_{Sr}}$ with a value of 0.39. Deviation of the *y*-axis intercept from zero is due to the precision of the measurement. The linearity in the slope of coccolith Sr/Ca implies that our experimental practice to adjust the Sr and Ca concentrations in our growth medium by changing either the strontium or the calcium concentration relative to those in natural seawater had no influence on the exchange coefficient.

The highest Sr/Ca applied in our experiments, 90 mmol mol^{-1}, was achieved by lowering the calcium concentration to 1 mmol L^{-1}. The corresponding calcite saturation state (Ω), with

$$\Omega = \frac{[Ca][CO_3]}{K_{sp}} \quad (7)$$

was 0.4, indicating undersaturation of seawater with respect to calcite. Scanning electron microscope (SEM) images of coccoliths produced under these conditions reveal partial dissolution of the rim and central area (Fig. 3). Therefore, the decreased calcification rate occurring at 1 mmol L^{-1} external Ca can in part be attributed to dissolution.

Cell growth rates and calcification rate of *E. huxleyi* varied between 0.32 and 0.91 d^{-1} and 2 and 58 pg calcite $cell^{-1}$ d^{-1} (see Table 3).

Discussion

Implications for proxy use—The Sr/Ca of *E. huxleyi* coccoliths increased linearly with increasing Sr/Ca of seawater within the range tested. This range comprised three orders of magnitude, and the lowest value corresponded to 1% of the modern seawater value. Because this range was much larger than the postulated changes of Sr/Ca in the seawater since the Cretaceous (Stoll and Schrag 2001; Lear et al. 2003), the assumption of a constant $K^{B}_{D_{Sr}}$ with changing sea-

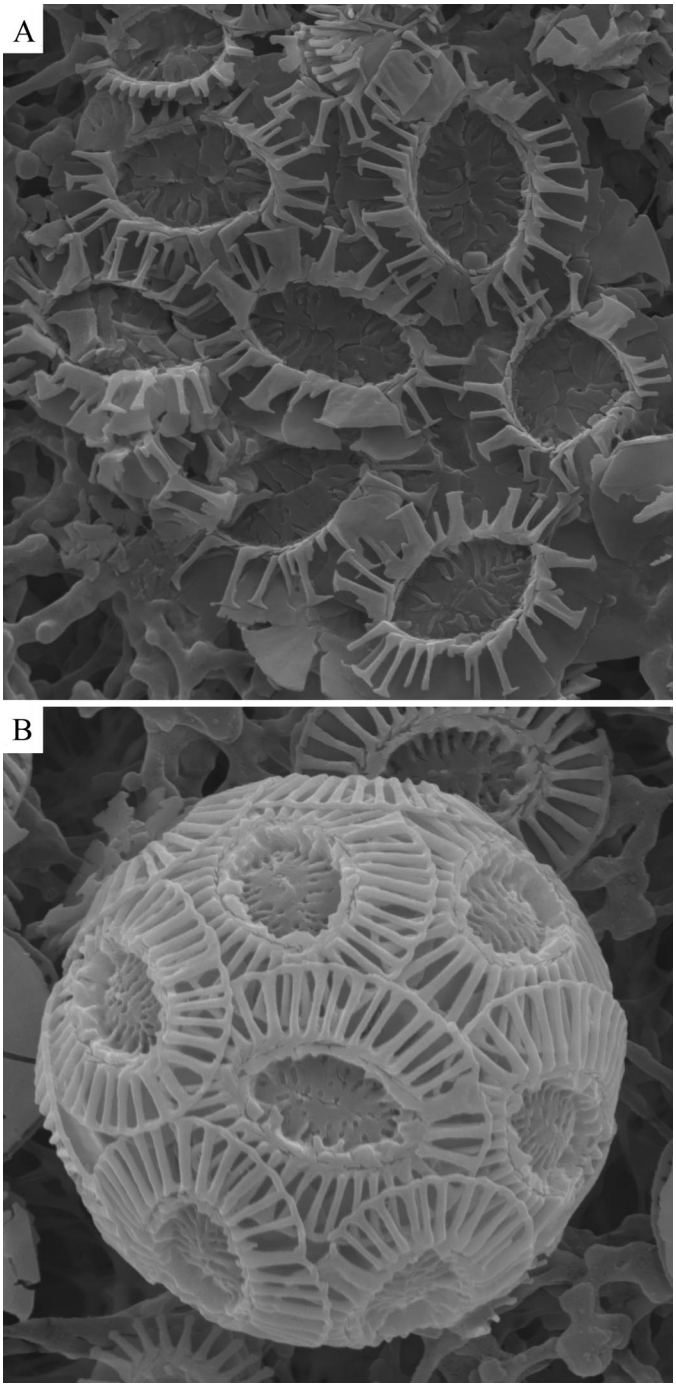

Fig. 3. SEM images of coccoliths produced under (A) 1 mmol L^{-1} Ca and (B) 10 mmol L^{-1} Ca in the bulk medium. The rim and central area show dissolution under 1 mmol L^{-1} Ca in the bulk medium.

water Sr/Ca (Stoll and Schrag 2001; Billups et al. 2004) is supported by the data presented here.

At 1 mmol L^{-1} external Ca, SEM images show partial dissolution of coccoliths, probably as a consequence of the calcite saturation state of 0.4. Lowered production of calcite is also likely to have occurred at 1 mmol L^{-1} calcium in seawater (Paasche 1964), an interpretation which the lower growth rates render even more likely. Consequently, we are not able to report the exact proportion of calcite that was subject to dissolution. However, the Sr/Ca of the remaining calcite fits the data obtained from coccoliths not showing partial dissolution. We conclude that partial dissolution seems to have no significant effect on coccolith Sr/Ca. This conclusion is supported by dissolution experiments with carbonate-rich sediment samples (Stoll and Schrag 2000). Furthermore, there are considerable differences in growth and calcification rates between the samples, which are the result of differences in light intensities (Table 3). Apparently these differences in growth and calcification rates have no effect on K^B_{DSr}. The confidence level ($r^2 = 0.99$) of the linear regression curve (Fig. 2) indicates a constant K^B_{DSr} with changing seawater Sr/Ca. This is in accord with previous experiments with *E. huxleyi* (Stoll et al. 2002*b*) and other species (Stoll et al. 2002*c*), which showed that irradiance-induced changes in growth rate did not affect strontium partitioning. Nutrient-stimulated changes in growth rate, on the other hand, affected strontium partitioning in *E. huxleyi* (Rickaby et al. 2002). This distinction between irradiance-induced and nutrient-stimulated changes in growth rate strongly suggests that some physiological processes, rather than growth rate per se, are responsible for variable strontium partitioning in coccoliths.

K^B_{DSr} *values of coccolithophore calcite*—The measured K^B_{DSr} of 0.39 falls well within the range of previously reported values (Rickaby et al. 2002; Stoll et al. 2002*b*). K^B_{DSr} values ranging from 0.1 to 0.6, depending on calcification rate, were measured by Rickaby et al. (2002) using the same strain as in our experiments. A different strain was used by Stoll et al. (2002*b*). Based on the data they published (seawater Sr/Ca 8.55 mmol mol^{-1}, coccolith Sr/Ca 2.92 mmol mol^{-1}), we calculated a K^B_{DSr} of 0.34.

Inorganically precipitated calcite shows K^D_{Sr} values ranging from 0.021 to 0.14 depending on the precipitation rate (Lorens 1981; Tesoriero and Pankow 1996), where the lowest value represents the thermodynamical equilibrium value. This value, however, is one order of magnitude smaller than the common K^B_{DSr} value for coccolith calcite (*see above*).

A positive correlation between K^B_{DSr} and growth rate is well documented for inorganically precipitated calcite (Lorens 1981; Tesoriero and Pankow 1996). The correlation was used by Carpenter and Lohmann (1992) in order to explain the high K^B_{DSr} of biogenic calcite. This hypothesis was examined with regard to coccolithophore calcite by Stoll et al. (2002*b*). The authors used a surface enrichment model (Watson and Liang 1995) to fit the above-mentioned data from inorganic precipitation experiments (Lorens 1981; Tesoriero and Pankow 1996). As concluded by the authors themselves, the calculations of Stoll et al. (2002*b*) show that K^B_{DSr} values of coccolith calcite cannot be explained by kinetic effects (i.e., simply by virtue of fast crystal growth rates). We perfectly agree with this conclusion, which is even underscored when considering the inevitable conversion of crystal growth rate units of the inorganic data (Tesoriero and Pankow 1996) in more detail. The relationship between seed crystal surface area and seed mass (i.e., the specific surface area) is the crucial number in this conversion. A careful review of the experiments described in Tesoriero and Pankow (1996) revealed that the value for specific surface area most likely is smaller than the one reported by Tesoriero and Pankow (1996). We put emphasis on the notion that this has no consequences at all for the results of Tesoriero and Pankow (1996). It has, however, consequences for K^B_{DSr} values of coccolith calcite, which can be obtained using this number. Given a linear coccolith growth rate of ca. 1×10^{-8} cm s^{-1} (Stoll et al. 2002*b*), a specific surface area of 0.1 m^2 g^{-1} (the value given by Tesoriero and Pankow [1996] is 0.6 m^2 g^{-1}) yields a K^B_{DSr} for coccolith calcite of 0.021, which represents the thermodynamical equilibrium value (Tesoriero and Pankow 1996). This calculation adds to the conclusion of Stoll et al. (2002*b*) that kinetic surface enrichment effects cannot explain the strontium partitioning in coccoliths.

Stoll et al. (2002*b*) also stated that the Sr/Ca of the coccolith vesicle solution is not known and that higher Sr/Ca of the calcifying fluid in comparison to seawater could possibly explain K^B_{DSr} values. A mechanism that produces such elevated Sr/Ca of coccolith vesicle solution is still lacking.

Toward an explanation of coccolith K^B_{DSr}*: A conceptual model*—In order to understand why intracellular Sr/Ca should differ from seawater ratio, it is necessary to briefly review the present knowledge of the calcification mechanism and cellular transport of calcium ions in *E. huxleyi.*

Precipitation of calcite takes place within a membrane-delimited space completely isolated from the cytosol, the coccolith vesicle (e.g., Young et al. 1999). Thus, seawater is separated from the site of calcification by at least two membranes, the plasma membrane and the coccolith-vesicle membrane. Calcium uptake for calcification is thought to be accomplished by transmembrane transport via Ca channels in the plasma membrane and Ca ATPases in the endomembrane system (Brownlee et al. 1995). It is still a matter of debate which compartment takes up calcium from the cytosol. It was suggested that the peripheral endoplasmic reticulum (ER) could play that role (Berry et al. 2002). Another structure that appears to be suited for the task is the reticular body, which is part of the coccolith vesicle in *E. huxleyi,* because this structure combines large surface area with small volume (Marsh 2000). For reasons of simplicity, we assume the reticular body to be responsible for Ca uptake from the cytosol in our further discussion. Another premise of our conceptual model is the small volume of solution surrounding the coccolith inside the coccolith vesicle. The membrane of the coccolith vesicle closely envelopes the growing coccolith and therefore does not contain a substantial reservoir of fluid. Judging from transmission electron micrographs, the vesicle volume is at most double the coccolith volume (Young and Henriksen pers. comm.) and is here assumed to have a maximum value of 1.8 μm^3.

Calcium homeostasis is accomplished by an arrangement

Table 4. Model parameters.

Parameter	Symbol	Unit	Values	References
Calcification rate	P	pg calcite cell^{-1} d^{-1}	50	Typical value (e.g., own results); Riebesell et al. 2000; Stoll et al. 2002*b*; Zondervan et al. 2002; Zondervan et al. 2001
Light : Dark cycle	L : D	1	16 : 8	Experimental setup
$CaCO_3$ content of one coccolith	$P_{\text{coccolith}}$	pg	2.2	Young and Ziveri 2000
Sr exchange coefficient	$K_{D_{Sr}}$	1	0.021	Tesoriero and Pankow 1996
Volume of coccolith vesicle solution	V	μm^3	1.8	Young and Henriksen pers. comm.
Ca precipitation flux	f_{Pr}^{Ca}	pmol h^{-1}	0.031	Calculated
Apparent Sr exchange coefficient	$K_{D_{Sr}}^{B}$	1	0.39 0.4	Experiment result; model result
Ca concentration in the coccolith vesicle	$[Ca]_{Sat}$	μmol L^{-1}	500	Meldolesi and Pozzan 1998
Ca concentration in seawater	$[Ca]_S$	mmol L^{-1}	10	Broecker and Peng 1982
Calcite saturation product in seawater	K_{sp}	mol^2 kg^{-2}	$10^{-6.37}$	Mucci 1983
Free energy change for ATP hydrolysis	ΔG	kcal mol^{-1}	15	Meldolesi and Pozzan 1998

of channels and pumps in the plasma membrane and various endomembranes that provides a steep calcium gradient between the cytosol and its environment. From a thermodynamical point of view, a Ca gradient of 10^4–10^5 can be achieved by the hydrolysis of ATP for a high ATP/ADP $\times$ Pi ratio in the cytosol, with a ΔG of 15 kcal mol^{-1} (Meldolesi and Pozzan 1998), and as a result of the presence of macromolecules (acidic polysaccharides, proteins) near the cell surface and probably also in the ER. The polysaccharides may form complexes with Ca or Sr, as known for calreticulin, thereby decreasing the concentration of the free cations.

The cytosolic concentration of Ca is a rather universal constant in the inactivated cell, with a value of 0.1 μmol L^{-1} (Brownlee et al. 1995). In the case that Ca pumps in the plasma membrane work near the thermodynamical limit, the gradient of 10^5 yields a calcium concentration of 10 mmol L^{-1} at the cell surface, which in fact is exactly the Ca concentration of seawater. Because of the calcium homeostasis, the Ca at the cell surface should be quite independent from the bulk Ca concentration in different experimental conditions. Ca transport near the thermodynamical limit would have the advantage that (1) pumping Ca from the cytosol to the environment proceeds with a minimum dissipation of energy in ATP consumption, and (2) a steep Ca gradient provides fast influx in cell signaling. We therefore postulate that a constant concentration of Ca at the cell surface represents a part of calcium homeostasis. The value of the surface Ca concentration we assume to be close to the thermodynamical limit (i.e., close to the Ca concentration of seawater, 10 mmol L^{-1}).

Calcification takes place in vesicles derived from the Golgi system. The kinetics of calcite formation can be optimized inside the cell, but biomineralization cannot bypass thermodynamics (e.g., calcite precipitation cannot occur below the calcite saturation concentration). Here we assume that thermodynamics is the only restriction for the vesicle calcification (i.e., the Ca concentration in the vesicle is determined by the saturation product). Hence, the calcite precipitation should start right after a supersaturation is obtained in the coccolith vesicle (see also Young et al. 1999). Moreover, the incorporation of Sr into calcite should proceed with the equilibrium $K_{D_{Sr}}$ of 0.021 (Tesoriero and Pankow 1996).

For an unconstrained inorganic precipitation of calcite in the coccolith vesicle, there are two possible scenarios for explaining the observed $K_{D_{Sr}}^{B}$. The first scenario is as follows: Precipitation occurs in steady state for both Ca and Sr. Under this condition the Sr/Ca of the calcite is determined by the ratio of the Sr and Ca influx. In this case the observed $K_{D_{Sr}}^{B} < 1$ could be explained in terms of a strong fractionation of the Ca pump against Sr. However, there is no experimental evidence for a significant difference in the cellular transport kinetics for Ca and Sr for either pumps (SERCA) nor channels (Allen and Sanders 1994; Berman and King 1990). Therefore, an unconstrained inorganic precipitation mechanism that operates in steady state appears to be unlikely.

In the second scenario, Sr/Ca of the new calcite is changing with time. The calcite precipitation yields an accumulation of Sr in the coccolith vesicle (owing to $K_{D_{Sr}} < 1$) until steady state is achieved. Then, the observed Sr/Ca of the coccolith calcite would be an integral value that arises from the sum of Sr/Ca over the time required for the formation of one coccolith. This mechanism assumes a similar timescale for reaching steady state and formation of the coccolith. The time required to achieve steady state can be estimated by means of a one-compartment model for inorganic precipitation of calcite in the coccolith vesicle. Within this model the concentrations of Ca and Sr in the vesicle are described in terms of two simple differential equations:

$$V\frac{d[\text{Ca}]}{dt} = f_{\text{In}}^{\text{Ca}} - f_{\text{Pr}}^{\text{Ca}}$$

$$V\frac{d[\text{Sr}]}{dt} = R^B f_{\text{In}}^{\text{Ca}} - K_{D_{\text{Sr}}}\frac{[\text{Sr}]}{[\text{Ca}]} f_{\text{Pr}}^{\text{Ca}}, \qquad R^B = \left(\frac{\text{Sr}}{\text{Ca}}\right)_{\text{bulk}}, \quad (8)$$

where V, $f_{\text{In}}^{\text{Ca}}$, and $f_{\text{Pr}}^{\text{Ca}}$ are coccolith vesicle volume, Ca influx, and Ca precipitation flux, respectively. In this model we assume that the ratio of the Sr and Ca influx equals the Sr/Ca in the bulk medium (R^B). Typical parameter values for the coccolith vesicle volume and the calcification rate are given in Table 4. After the onset of calcite precipitation, the Ca

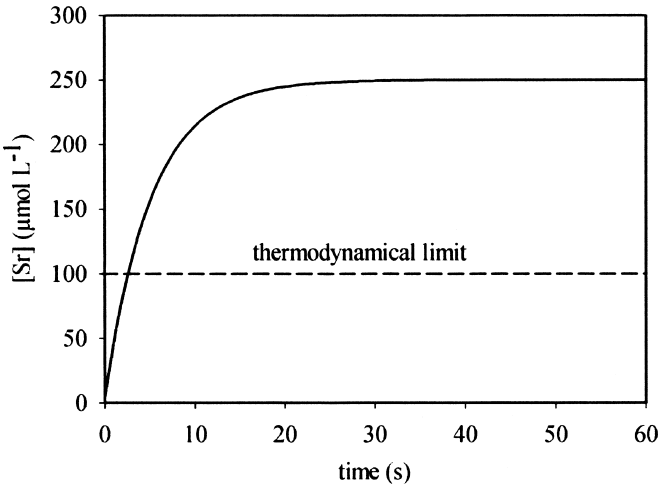

Fig. 4. Concentration of Sr in the coccolith vesicle. The solid curve shows the increase of Sr concentration after onset of calcite precipitation as it would follow from an unconstrained inorganic precipitation mechanism. The dashed line indicates the thermodynamical limit imposed by the Ca pump in the coccolith vesicle membrane. Shown are the values corresponding to a bulk medium Sr/Ca of 0.01 (i.e., the Sr/Ca of seawater).

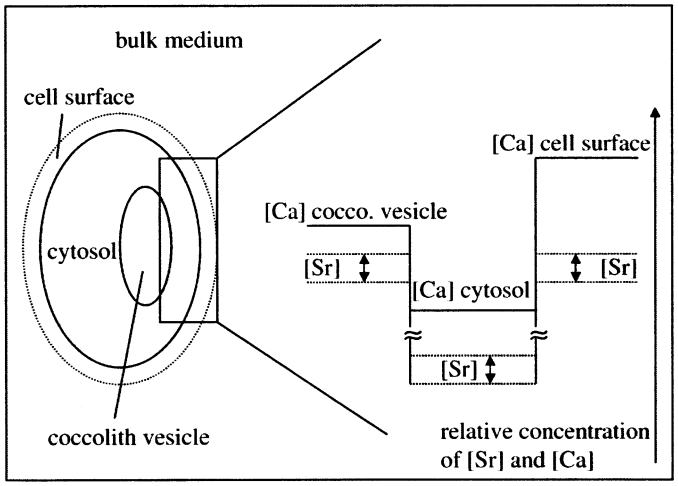

Fig. 5. Proposed mechanism for the partitioning of Sr and Ca during calcification in *E. huxleyi* yielding the $K^{B}_{D_{Sr}}$. Depicted are the relative concentrations of Sr and Ca in the two involved cellular compartments (coccolith vesicle and cytosol) and the cell surface (schematic drawing). The Sr concentration (dashed lines) at the cell surface and in the coccolith vesicle increases until the thermodynamical limit of the concentration gradient between the cytosol and adjacent compartments is reached. The same holds for the Ca concentration (solid lines) at the cell surface. On the other hand, the Ca concentration in the coccolith vesicle is determined by the saturation product. All variations of the Sr concentration at the cell surface are reflected by variations of the Sr concentration in the coccolith vesicle (as indicated by the double-headed arrows).

concentration in the coccolith vesicle is assumed to be constant, where the value of Ca concentration is determined by the saturation product. Then the solution of Eq. 8 yields the following expression for the time dependence of the Sr concentration:

$$[\mathrm{Sr}] = [\mathrm{Ca}]_{\mathrm{Sat}} \frac{R^B}{K_{D_{\mathrm{Sr}}}} [1 - (1 - K_{D_{\mathrm{Sr}}}) e^{-t/\tau}], \tag{9}$$

where the characteristic time constant, τ, is given by

$$\tau = \frac{V}{K_{D_{\mathrm{Sr}}}} \frac{[\mathrm{Ca}]_{\mathrm{Sat}}}{f^{\mathrm{Ca}}_{\mathrm{Pr}}} = 5.2 \text{ s}. \tag{10}$$

The value of τ indicates that the steady state is obtained after a few seconds, which is negligible compared with the 0.7 h required for the formation of one coccolith. Thus, the $K^{B}_{D_{Sr}}$ of coccolith calcite is entirely determined by its steady state value. Therefore, also we need to exclude the second scenario as a possible mechanism yielding the observed coccolith $K^{B}_{D_{Sr}}$.

Based on the previous discussion, we speculate that there is a strong impact of the cell physiology on the coccolith Sr/Ca. We suggest that the Ca pumps in the endomembrane system provide an additional thermodynamical constraint on inorganic calcite precipitation: During the calcification, the concentration of Sr in the coccolith vesicle increases with time (*see Eq. 9 and Fig. 4*). However, the accumulation of Sr in the vesicle will stop at the thermodynamical limit existing for the gradient of Sr concentration between the vesicle and the cytosol (*see Fig. 4*). At the thermodynamical limit, a gradient of 10^5 between the cytosol and the coccolith vesicle can be expected for Sr, corresponding to the situation at the plasma membrane.

Hence, the achieved Sr concentration in the vesicle ($[\mathrm{Sr}]_V$) is smaller than the steady state concentration of an unconstrained inorganic precipitation and should be close to the Sr concentration at the cell surface ($[\mathrm{Sr}]_S = [\mathrm{Sr}]_V$). Therefore, we assume that $[\mathrm{Sr}]_V$ mirrors all changes of $[\mathrm{Sr}]_S$, whereas the value of the Ca concentration in the vesicle ($[\mathrm{Ca}]_V$) is close to the saturation value ($[\mathrm{Ca}]_{Sat}$; *see Fig. 5*). Since the external CO_2 concentrations are the same for all of our experiments, $[\mathrm{Ca}]_{Sat}$ should be constant. Also, the Ca concentration at the cell surface ($[\mathrm{Ca}]_S$) is assumed to be a constant (10 mmol L^{-1}) owing to Ca homeostasis (see above). Then, in the expression for the $K^{B}_{D_{Sr}}$ of coccolith calcite, the Sr concentrations in the coccolith vesicle and at the cell surface cancel

$$K^{B}_{D_{\mathrm{Sr}}} = K_{D_{\mathrm{Sr}}} \frac{[\mathrm{Sr}]_V}{[\mathrm{Ca}]_V} \frac{[\mathrm{Ca}]_B}{[\mathrm{Sr}]_B} = K_{D_{\mathrm{Sr}}} \frac{[\mathrm{Sr}]_V}{[\mathrm{Ca}]_{\mathrm{Sat}}} \frac{[\mathrm{Ca}]_S}{[\mathrm{Sr}]_S}$$

$$= K_{D_{\mathrm{Sr}}} \frac{[\mathrm{Ca}]_S}{[\mathrm{Ca}]_{\mathrm{Sat}}} = \text{constant}. \tag{11}$$

Hence, we conclude that the $K^{B}_{D_{Sr}}$ of coccolith calcite should have a constant value, given a constant external CO_2 concentration. This is in good agreement with our experimental finding.

Using for $[\mathrm{Ca}]_{Sat}$ a typical value for [Ca] in the ER (500 μmol L^{-1}; *see Table 4*) yields a $K^{B}_{D_{Sr}}$ of 0.4, which is very close to the observed $K^{B}_{D_{Sr}}$ of 0.39. Based on the seawater saturation product ($K_{sp} = 10^{-6.37}$ mol^2 kg^{-2}; *see Table 4*), a $[\mathrm{Ca}]_{Sat}$ of 500 μmol L^{-1} would correspond to a [DIC] in the vesicle (or $[CO_3^{2-}]$ at a strong alkaline pH) of 893 μmol L^{-1}.

This is probably a slightly overestimated value for [DIC] in the vesicle, because the ionic strength inside the coccolith vesicle is most likely lower than that of seawater (Anning et al. 1996). However, a [DIC] of 893 μmol L^{-1} is still in agreement with the observed mean cellular DIC of 500 μmol L^{-1} (Anning et al. 1996).

As mentioned above, previous experiments with *E. huxleyi* (Stoll et al. 2002*b*) and other species (Stoll et al. 2002*c*) showed that irradiance-induced changes in growth rate did not affect strontium partitioning, whereas nutrient-stimulated changes did (Rickaby et al. 2002). Since *E. huxleyi* does not dispose of an efficient nitrogen uptake system (Riegman et al. 2000), it is possible that nitrogen availability affects DIC transport proteins. If DIC concentration in the coccolith vesicle and external nitrogen concentration are positively correlated, this would have an effect on strontium partitioning. According to our model, an increase in coccolith vesicle DIC concentration corresponds to a decrease in coccolith vesicle calcium concentration $[Ca]_{Sat}$. Hence an increase in external nitrogen concentration would lead to an increase in $K^B_{D_{Sr}}$ predicted by our model (Eq. 11). This correlation was observed experimentally (Rickaby et al. 2002). In the latter study, $K^B_{D_{Sr}}$ values ranging from 0.1 to almost 0.7 were measured. In order to cover this range in our model, values for $[Ca]_{Sat}$ ranging from 279 μmol L^{-1} to 1,950 μmol L^{-1} are required. These values fall well within the range of measured ER values (Meldolesi and Pozzan 1998). An additional explanation for effects of nitrogen limitation can be given. Under nitrogen limitation, *E. huxleyi* produces excess polysaccharides, which are extruded onto the cell surface (Engel et al. 2004). Polysaccharides bind divalent cations by a complex mechanism called the egg-box model (Pellerin and O'Neill 1998), where strontium is bound more strongly to polysaccharides than to calcium (Cohen-Shoel et al. 2002). Hence with increasing polysaccharide concentration at the cell surface, the calcium to strontium ratio at the cell surface would also increase and become higher than that of the bulk medium. Mathematically this can be described by adding a factor γ to Eq. 11:

$$K^B_{D_{Sr}} = K_{D_{Sr}} \frac{[Sr]_V}{[Ca]_V} \frac{[Ca]_B}{[Sr]_B} = K_{D_{Sr}} \gamma \frac{[Sr]_V}{[Ca]_{Sat}} \frac{[Ca]_S}{[Sr]_S}$$

$$= K_{D_{Sr}} \gamma \frac{[Ca]_S}{[Ca]_{Sat}} \quad (12)$$

The factor γ can assume values between 0 and 1. In the case of no polysaccharides at the cell surface, $\gamma = 1$. It should be noted that a very small amount of polysaccharides, the coccolith-associated polysaccharides (CAP; Henriksen et al. 2004), is always present at the cell surface of *E. huxleyi*. The amount of CAP, however, is negligible compared with the amount of polysaccharides produced and extruded additionally during nitrogen limitation (Engel et al. 2004).

Strontium partitioning in different coccolithophore species is not the same under identical conditions; $K^B_{D_{Sr}}$ values range from 0.257 to 0.356 among five species at 17°C (Stoll et al. 2002*a*). According to our model, this corresponds to a range of coccolith vesicle calcium concentrations $[Ca]_{Sat}$ from 548 to 759 μmol L^{-1}. We propose that different species (or strains) have different coccolith vesicle calcium concentrations and that this is the reason why $K^B_{D_{Sr}}$ values differ among species (or strains). One explanation for species-specific coccolith vesicle calcium concentrations is that different species have different polysaccharides in the coccolith vesicle (Marsh 2000), which in turn requires different coccolith vesicle calcium concentrations $[Ca]_{Sat}$ in order to achieve supersaturation with respect to calcite.

The capability of the model can be further demonstrated by applying it to two independent data sets. The first set of data describes the temperature dependence of $K^B_{D_{Sr}}$ in *E. huxleyi* (Stoll et al. 2002*b*), whereas the second shows the temperature dependence of $K_{D_{Sr}}$ in inorganic calcite precipitation experiments (Malone and Baker 1999). Both data sets show a linear dependence of the Sr incorporation into calcite. However, the two slopes differ by one order of magnitude. Inserting the expression for the dependence of $K_{D_{Sr}}$ obtained from inorganic precipitation experiments (slope, 1.85×10^{-4} $°C^{-1}$) into Eq. 11 yields the $K^B_{D_{Sr}}$ for Sr incorporation into *E. huxleyi* coccoliths with a slope of 3.7×10^{-3} $°C^{-1}$. This model value is in agreement with the observed slope of 3.2×10^{-3} $°C^{-1}$ (Stoll et al. 2002*b*).

We have shown experimentally that coccolith Sr/Ca of *E. huxleyi* increases linearly with increasing seawater Sr/Ca over three orders of magnitude. This relationship, in general, provides the basis for correcting measured Sr/Ca from sediment samples for different composition of seawater with respect to these ions.

The high $K^B_{D_{Sr}}$ values measured for coccolith calcite can be explained by a simple conceptual model based on the channel/carrier-mediated transport of calcium and strontium ions inside the cell. The model is solely based on thermodynamical constraints and does not assume a relationship between the exchange coefficient and the crystal growth rate.

References

Allen, G. J., and D. Sanders. 1994. Two voltage-gated, calcium release channels coreside in the vacuolar membrane of broad bean guard cells. Plant Cell **6:** 685–694.

Anning, T., N. Nimer, M. J. Merrett, and C. Brownlee. 1996. Costs and benefits of calcification in coccolithophorids. Journal of Marine Systems **9:** 45–56.

Beattie, P., and others. 1993. Terminology for trace-element partitioning. Geochimica et Cosmochimica Acta **57:** 1605–1606.

Berman, M. C., and S. B. King. 1990. Stoichiometries of calcium and strontium transport coupled to ATP and acetyl phosphate hydrolysis by skeletal sarcoplasmic reticulum. Biochim. Biophys. Acta—Biomembranes **1029:** 235–240.

Berry, L., A. R. Taylor, U. Lucken, K. P. Ryan, and C. Brownlee. 2002. Calcification and inorganic carbon acquisition in coccolithophores. Functional Plant Biology **29:** 289–299.

Billups, K., R. E. M. Rickaby, and D. P. Schrag. 2004. Cenozoic pelagic Sr/Ca records: Exploring a link to paleoproductivity. Paleoceanography **19:** doi:1029/2004PA001011.

Bradshaw, A. L., P. G. Brewer, D. K. Shaffer, and R. T. Williams. 1981. Measurements of total carbon dioxide and alkalinity by potentiometric titration in the GEOSECS program. Earth and Planetary Science Letters **55:** 99–115.

Brewer, P. G., A. L. Bradshaw, and R. T. Williams. 1986. Measurement of total carbon dioxide and alkalinity in the North Atlantic ocean in 1981, p. 358–381. *In* J. R. Trabalka and D.

E. Reichle [eds.], The changing carbon cycle—a global analysis. Springer Verlag.

BROECKER, W. S., AND T. PENG. 1982. Tracers in the sea, 1st ed. Lamont-Doherty Geological Observatory, Columbia University.

BROWNLEE, C., M. DAVIES, N. NIMER, L. F. DONG, AND M. J. MERRETT. 1995. Calcification, photosynthesis and intracellular regulation in *Emiliania huxleyi.* Bulletin de l' Institut oceanographique, Monaco n' special **14:** 19–35.

CARPENTER, S. J., AND K. C. LOHMANN. 1992. Sr/Mg ratios of modern marine calcite: Empirical indicators of ocean chemistry and precipitation rate. Geochimica et Cosmochimica Acta **56:** 1837–1849.

COHEN-SHOEL, N., D. ILZYCER, I. GILATH, AND E. TEL-OR. 2002. The involvement of pectin in Sr^{2+} biosorption by *Azolla*. Water Air Soil Poll. **135:** 195–205.

DICKSON, A. G., AND F. J. MILLERO. 1987. A comparison of the equilibrium constants for the dissociation of carbonic acid in seawater media. Deep-Sea Research **34:** 1733–1743.

ENGEL, A., AND OTHERS. 2004. Transparent exopolymer particles and dissolved organic carbon production by *Emiliania huxleyi* exposed to different CO_2 concentrations: A mesocosm experiment. Aquatic Microbial Ecology **34:** 93–104.

GRAN, G. 1952. Determination of the equivalence point in potentiometric titrations of seawater with hydrochloric acid. Oceanologica Acta **5:** 209–218.

GUILLARD, R. R. L., AND J. H. RYTHER. 1962. Studies of marine planktonic diatoms, I, *Cyclotella nanna* (Hustedt) and *Detonula convervacea* (Cleve). Can. J. Microbiol. **8:** 229–239.

HENRIKSEN, K., S. L. S. STIPP, J. YOUNG, AND M. E. MARSH. 2004. Biological control on calcite crystallization: AFM investigation of coccolith polysaccharide function. American Mineralogist **89:** 1586–1596.

LEAR, C. H., H. ELDERFIELD, AND P. A. WILSON. 2003. A Cenozoic seawater Sr/Ca record from benthic foraminiferal calcite and its application in determining global weathering fluxes. Earth and Planetary Science Letters **208:** 69–84.

LEWIS, E., AND D. W. R. WALLACE. 1998. Program developed for CO_2 system calculations ORNL/CDIAC-105. Carbon Dioxide Information Analysis Centre, Oak Ridge National Laboratory, U.S. Department of Energy.

LORENS, R. B. 1981. Sr, Cd, Mn, and Co distribution coefficients in calcite as a function of calcite precipitation rate. Geochimica et Cosmochimica Acta **45:** 553–561.

MALONE, M. J., AND P. A. BAKER. 1999. Temperature dependence of the strontium distribution coefficient in calcite: An experimental study from 40° to 200°C and application to natural diagenetic calcites. Journal of Sedimentary Research **69:** 216–223.

MARSH, M. E. 2000. Polyanions in the $CaCO_3$ mineralization of coccolithophores, p. 251–268. *In* E. Baeuerlein [ed.], Biomineralization: From biology to biotechnology and medical application. Wiley-VCH.

MCINTIRE, W. L. 1963. Trace element partition coefficients—a review of theory and applications to geology. Geochimica et Cosmochimica Acta **27:** 1209–1264.

MEHRBACH, C., C. H. CULBERSON, J. E. HAWLEY, AND R. M. PYTKOVICZ. 1973. Measurement of the apparent dissociation constants of carbonic acid in seawater at atmospheric pressure. Limnol. Oceanogr. **18:** 897–907.

MELDOLESI, J., AND T. POZZAN. 1998. The endoplasmic reticulum Ca^{2+} store: A view from the lumen. Trends Biochem. Sci. **23:** 10–14.

MUCCI, A. 1983. The solubility of calcite and aragonite in seawater at various salinities, temperatures and one atmosphere total pressure. American Journal of Science **283:** 780–799.

NIELSEN, A. E. 1964. Kinetics of precipitation. Pergamon Press.

PAASCHE, E. 1964. A tracer study of the inorganic carbon uptake during coccolith formation and photosynthesis in the coccolithophorid *Coccolithus huxleyi*. Physiol. Plant. **Supplementum III:** 1–82.

PELLERIN, P., AND M. A. O'NEILL. 1998. The interaction of the pectic polysaccharide Rhamnogalacturonan II with heavy metals and lanthanides in wines and fruit juices. Analusis Magazine **26:** 32–36.

RICKABY, R. E. M., D. P. SCHRAG, I. ZONDERVAN, AND U. RIEBESELL. 2002. Growth rate dependence of Sr incorporation during calcification of *Emiliania huxleyi*. Global Biochemical Cycles **16:** doi:1029/2001GB001408.

RIEBESELL, U., I. ZONDERVAN, B. ROST, P. D. TORTELL, R. E. ZEEBE, AND F. M. M. MOREL. 2000. Reduced calcification of marine plankton in response to increased atmospheric CO_2. Nature **407:** 364–367.

RIEGMAN, R., W. STOLTE, A. A. M. NOORDELOOS, AND D. SLEZAK. 2000. Nutrient uptake and alkaline phosphatase (ec 3:1:3:1) activity of *Emiliania huxleyi* (Prymnesiophyceae) during growth under n and p limitation in continuous cultures. Journal of Phycology **36:** 87–96.

RIMSTIDT, J. D., A. BOLAG, AND J. WEBB. 1998. Distribution of trace elements between carbonate minerals and aqueous solutions. Geochimica et Cosmochimica Acta **62:** 1851–1863.

SMITH, S. V., R. W. BUDDEMEIER, R. C. REDALJE, AND J. E. HOUCK. 1979. Strontium-calcium thermometry in coral skeletons. Science **204:** 404–407.

STOLL, H. M., C. M. KLAAS, I. PROBERT, J. RUIZ ENCINAR, AND J. I. GARCIA ALONSO. 2002*a*. Calcification rate and temperature effects on Sr partitioning in coccoliths of multiple species of coccolithophorids in culture. Global and Planetary Change **34:** 153–171.

———, Y. ROSENTHAL, AND P. FALKOWSKI. 2002*b*. Climate proxies from Sr/Ca of coccolith calcite: Calibrations from continuous culture of *Emiliania huxleyi.* Geochimica et Cosmochimica Acta **66:** 927–936.

——— AND D. P. SCHRAG. 1998. Effects of quaternary sea level cycles on strontium in seawater. Geochimica et Cosmochimica Acta **62:** 1107–1118.

——— AND ———. 2000. Coccolith Sr/Ca as a new indicator of coccolithophorid calcification and growth rate. Geochemistry Geophysics Geosystems **1:** doi:10.1029/1999GC00015.

——— AND ———. 2001. Sr/Ca variations in Cretaceous carbonates: relation to productivity and sea level changes. Palaeogeography, Palaeoclimatology, Palaeoecology **168:** 311–336.

———, P. ZIVERI, M. GEISEN, I. PROBERT, AND J. YOUNG. 2002*c*. Potential and limitations of Sr/Ca ratios in coccolith carbonate: New perspectives from cultures and monospecific samples from sediments. Phil. Trans. R. Soc. Lond. A **360:** 719–747.

STOLL, M. H. C., K. BAKKER, G. H. NOBBE, AND R. R. HAESE. 2001. Continuous-flow analysis of dissolved inorganic carbon content in seawater. Anal. Chem. **73:** 4111–4116.

TESORIERO, A. J., AND J. F. PANKOW. 1996. Solid solution partitioning of Sr^{2+}, Ba^{2+}, and Cd^{2+} to calcite. Geochimica et Cosmochimica Acta **60:** 1053–1063.

WATSON, B., AND Y. LIANG. 1995. A simple model for sector zoning in slowly grown crystals: Implications for growth rate and lattice diffusion, with emphasis on accessory minerals in crustal rocks. American Mineralogist **80:** 1179–1187.

YOUNG, J. R., S. A. DAVIS, P. R. BOWN, AND S. MANN. 1999. Coccolith ultrastructure and biomineralisation. Journal of Structural Biology **126:** 195–215.

———, AND P. ZIVERI. 2000. Calculation of coccolith volume and

its use in calibration of carbonate flux estimates. Deep-Sea Research. **47:** 1679–1700.

ZONDERVAN, I., B. ROST, AND U. RIEBESELL. 2002. Effect of CO_2 concentration on the PIC/POC ratio in the coccolithophore *Emiliania huxleyi* grown under light-limiting conditions and different day lengths. J. Exp. Mar. Biol. Ecol. **272:** 55–70.

ZONDERVAN, I., R. E. ZEEBE, B. ROST, AND U. RIEBESELL. 2001. Decreasing marine biogenic calcification: A negative feedback on rising atmospheric pCO_2. Global Biogeochemical Cycles **15:** 507–516.

Received: 18 April 2005
Accepted: 10 August 2005
Amended: 15 September 2005